Journal of Power Sources xxx (2017) 1–7

Contents lists available at ScienceDirect

Journal of Power Sources

journal homepage: www.elsevier.com/locate/jpowsour

Performance of electro-spun carbon nanofiber electrodes with conductive poly(3,4-ethylenedioxythiophene) coatings in bioelectrochemical systems

Juan J.L. Guzman [a, 1], Meryem O. Pehlivaner Kara [b, 1], Margaret W. Frey [b], Largus T. Angenent [a, c, *]

[a] Department of Biological and Environmental Engineering, Cornell University, Ithaca, NY 14853, United States
[b] Department of Fiber Science and Apparel Design, Cornell University, Ithaca, NY 14853, United States
[c] Center for Applied Geosciences, University of Tübingen, 72074 Tübingen, Germany

HIGHLIGHTS

- PEDOT was successfully coated on polyacrylonitrile and carbonized nanofibers.
- PEDOT coating increased conductivity, capacitance, and current production in BESs.
- PEDOT coating increased the specific surface area for electrodes with a low area.
- PEDOT coating decreased the specific surface area for electrodes with a high area.
- PEDOT coating on a gold microfluidic electrode increased current almost 3 fold.

GRAPHICAL ABSTRACT

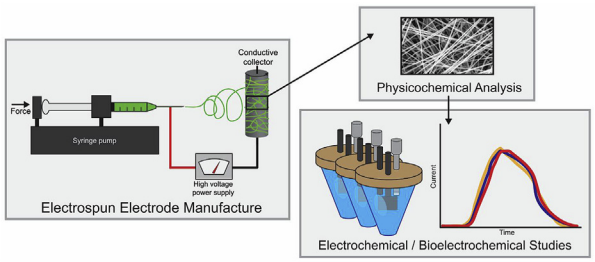

ARTICLE INFO

Article history:
Received 15 January 2017
Received in revised form
27 March 2017
Accepted 28 March 2017
Available online xxx

Keywords:
Electro-spun
Polyacrylonitrile
Carbon nanofiber
PEDOT
Bioelectrochemistry
Bioelectrochemical system

ABSTRACT

Bioelectrochemical systems (BESs) employ extracellular electron transfer from bacteria that grow at electrodes. Due to biofilm and electrode limitations, industrial-scale applications require large electrode areas, and thus inexpensive electrode materials. Here, electro-spun polyacrylonitrile (PAN) and carbon nanofiber (CNF) were manufactured. In addition, the conductive polymer poly(3,4-ethylenedioxythiophene) (PEDOT) was applied as a coating to these materials and to carbon cloth (CC). We tested these materials as electrodes by using physicochemical measurements, cyclic voltammetry, and bioelectrochemical growth-studies with *Geobacter sulfurreducens*. PAN is a nonconductive material without capacitance, but with PEDOT coating the conductivity and capacitance became sufficient to support electric current production in our BES. CNF outperformed CC in capacitance, but behaved similarly in our BES when normalized to projected surface area. With the PEDOT coating, CNF increased electric current production by 38% in our BES, while this was 64% for CC. When applied to a gold microfluidic electrode, electric current with *G. sulfurreducens* increased almost three-fold. PEDOT added considerable specific surface area to electrodes possessing a low

* Corresponding author. Hölderlingstr. 12, 72074 Tübingen, Germany.
E-mail address: l.angenent@uni-tuebingen.de (L.T. Angenent).
[1] Guzman and Pehlivaner Kara are first co-authors.

http://dx.doi.org/10.1016/j.jpowsour.2017.03.133
0378-7753/

surface area, but not with a high surface area such as CNF. This work demonstrates that electro-spun electrodes and PEDOT coating are a promising electrode alternative that can be readily implemented into existing BESs.

1. Introduction

Bioelectrochemical systems (BESs) are fuel-cell-architecture-based, clean-energy technologies that have shown promise for the simultaneous treatment of wastewater [1–6] and production of electrical energy [6,7], biogas [8,9], and value-chemicals [10]. BESs employ electrochemically active bacteria at the anode and/or cathode, which use extracellular electron transfer to and from electrodes. Most BES studies have focused on lab-scale systems, with some limited success with pilot systems [11]. An economically feasible BES at a true industrial-scale has been slow to emerge due to the high capital costs that are required to build the intricate architectures [11,12]. One limiting component that can drive high capital costs is the low current density of the microbiota, leading to the requirement of large projected surface areas for the electrodes and potentially membranes. Therefore, the scientists and engineers within the research area of microbial electrochemistry are trying to develop cost-effective electrode materials that will increase extracellular-electron-transfer rates between the microbiota and the electrode surface to minimize system size. Specifically, considerable research has focused on superior electrode materials that feature high conductivity, surface area, biocompatibility, and porosity.

Carbon materials have been widely used for electrodes because they are highly conductive and resistant to corrosion, and feature a high specific surface area. Various configurations of carbon electrodes, such as cloth, felt, brush, and paper, have been developed, achieving power densities in the 100 W m^{-3} range [13]. Recently, electro-spun carbon nanofiber (CNF) materials have been explored due to their high porosity, surface area density, biocompatibility, customizability, and ease of manufacture [14–17]. Notably, CNF features higher specific surface area and porosity compared to conventional electrodes including carbon cloth (CC) [18–20], carbon mesh [21,22], graphite [23], and carbon brush [24]. CNF can be produced by electro-spinning polyacrylonitrile (PAN), followed by stabilization and carbonization, and can be produced cost-competitive to CC [13,25,26].

To further improve these materials, surface functionalization with platinum catalysts and carbon powder has improved reaction rates, increasing performance four-fold [27]. However, platinum functionalization is expensive and becomes poisoned during operation in real-world environments. Carbon nanotube functionalization has been studied as an alternative to platinum, where it increased specific surface area, microbial interaction, mechanical properties, and conductivity, but costs were still high [18,28–30]. Conductive polymers have also been explored as coatings for electrodes because they combine the physical and chemical properties of organic polymers with the electrical properties of metals. They have shown promise for applications in the areas of flexible electronics, electrochromic displays, transistors, and capacitors [31–33]. For example, fluorinated polymers have been studied as BES electrode coatings, with 40-fold improvements in current production [34].

Poly(3,4-ethylenedioxythiophene) (PEDOT) has been studied as an electrode coating in electrochemical systems because of its high electrical conductivity at neutral pH, chemical stability, and high capacitance [35–38]. Coating electrodes with PEDOT can be achieved through *in-situ* interfacial polymerization [39] and electrochemical deposition [37]. *In-situ* interfacial polymerization offers the advantages of cost-effective and scalable production, and can be applied to nonconductive surfaces. Electrochemical deposition requires a conductive surface, but allows highly controlled PEDOT deposition on targeted areas, such as on microelectrodes. For these reasons, PEDOT has already been applied to commercially available electrodes such as CC and felt in microbial fuel cells (MFCs), where 10–50% increases in power production were observed [40–42]. While other catalysts have reported more dramatic increases in performance, their benefits had to be balanced out by their significant costs; the price for platinum catalyst, for example, is \$80 g^{-1}, as opposed to \$2 g^{-1} for PEDOT. The exact mechanism for the increased performance could not be elucidated, but capacitive electrodes have been shown to increase performance in BESs by 50% [25,43,44]. However, these studies focused on utilizing charge-discharge cycles to increase power harvesting rather than continuous performance.

Here, PAN pieces were manufactured through the electrospinning process, and subsequently converted into CNF electrodes through a carbonization process. The performance of electro-spun PAN and CNF, and CC electrode materials was tested with and without PEDOT as a conductive coating for bioelectrochemical applications by using physicochemical, electrochemical, and bioelectrochemical methods. Conductivity, fiber diameter, specific surface area, and porosity were measured, as well as Raman and FTIR spectroscopy. Cyclic voltammetry tests were performed to analyze electrochemical properties and to calculate capacitance. Next, these electrodes were utilized in BESs that were inoculated with *Geobacter sulfurreducens* PCA and operated chronoamperometrically in batch. Finally, we coated a gold electrode with PEDOT for a specialized microelectrode application and measured current densities with *G. sulfurreducens* PCA.

2. Experimental

2.1. PAN electro-spinning, CNF synthesis, and PEDOT deposition

10% wt. PAN solution was electro-spun at 0.5 mL h^{-1} and 17 kV onto a sheet. The sheet was cut to make electrodes with projected surface areas of 2.0 cm × 1.7 cm, stabilized in air at 270 °C for 1 h, then carbonized in a nitrogen atmosphere at 1000 °C for 20 min (Supplemental materials [SM]). Ramp rates for the stabilization and carbonization processes were 1 and 5 °C min^{-1}, respectively. Electrode substrates were immersed in a solution of EDOT-$FeCl_3$ in ethanol (EDOT: 0.05 g mL^{-1}, $FeCl_3$: 0.05 g mL^{-1}) and allowed to polymerize to PEDOT. After polymerization, samples were cleaned with methanol *via* ultrasonic oscillation for 20 min. Finally, coated materials were dried under vacuum overnight.

2.2. Fiber characterization

Nanofiber morphology was observed by sputter coating materials with gold-palladium *prior* to examination with a scanning electron microscope (SEM) (Leica 440, Wetzlar, Germany). Average

Please cite this article in press as: J.J.L. Guzman, et al., Journal of Power Sources (2017), http://dx.doi.org/10.1016/j.jpowsour.2017.03.133

fiber diameter was determined from SEM images using open-source ImageJ software. The extent of carbonization was determined using a Magna 560 FTIR spectrometer (Nicolet Instrument Corp., Madison, WI, USA). A 1100-AEHXL capillary flow porometer (Porous Media Inc., Ithaca, NY, USA) was used to measure the mean pore size using Solwick wetting agent (Porous Media Inc.) with a defined surface tension of 20.1 dyn cm^{-1}. BET surface area (specific surface area) measurements were performed in a Gemini VII 2390t (Micrometrics Instrument Corp., Atlanta, GA, USA) using ultra-high purity liquid nitrogen. PEDOT deposition was probed by Raman spectroscopy with a 785-nm laser source. Conductivity was measured using the four-point probe method (ASTM 4496-04) with a digital multimeter (Model 2400, Keithley Instruments, Cleveland, OH, USA). The conductivity of each sample was measured ten times in different directions; the mean and standard error values were reported.

2.3. Cyclic voltammetry (CV)

CV tests were performed in triplicate with an Electrochemical Analyzer 600B (CH Instruments, Austin, TX, USA) with the following settings: five cycles, scan rate of 25 mV s^{-1}, and potential range of −0.4–1.0 V (*vs.* Ag/AgCl). CV tests were performed in an electrochemical cell (CHI220, CH Instruments) filled with 5 mM potassium ferricyanide and 200 mM sodium sulfate. A new solution was introduced into the cell for each test and was aggressively sparged with 80%:20% N_2:CO_2 gas in excess of 15 min. During the CV test, the gas-sparging level was lifted into the headspace to maintain anaerobic conditions for the duration without disrupting the measurement. The cell used an Ag/AgCl/sat'd KCl reference electrode manufactured in-house and a 4.76-mm diameter fine extruded graphite rod (Graphite Store, Buffalo Grove, IL, USA) counter electrode. 1 cm × 1 cm test electrodes were fixed to identical rods using conductive carbon cement (CCC, Electron Microscopy Sciences, Hatfield, PA, USA). We calculated capacitance values from the CV curves [45] (SM).

2.4. Bioelectrochemical growth tests

We performed bioelectrochemical growth tests in triplicate using an open-source BES reactor design [46] based on a previously published study [47]. We also used the same reference and counter electrodes as in the CV setup. The test electrodes were fixed to graphite rods with carbon cement, and a clear nail polish (Clear Ice 004, Cover Girl, Baltimore, MD, USA) was applied to the bottom 2 cm as insulation from the electrolyte during the extended growth experiments. The bioreactors were autoclaved, filled with 15 mL of sterile growth media with 40 mM sodium acetate, placed in a 30 °C water bath, constantly stirred at 110 rpm, and sparged with 80%:20% N_2:CO_2 gas (SM). The electrodes were connected to a multichannel potentiostat (VSP, Biologic Science Instruments, Claix, France) and operated chrono-amperometrically at +0.3 V (vs. Ag/AgCl), and interrupted daily for diagnostic CVs. The bioreactors were inoculated with 1 mL of 0.1 OD *G. sulfurreducens* PCA within 24 h of setup (SM).

3. Results and discussion

3.1. Electro-spun materials have small fiber diameters and high specific surface areas

One of the expectations of this study was that using small fiber diameters, which are formed by electro-spun PAN, would provide high specific surface area for microbial colonization, allowing increased electron transfers. In addition, carbonization of PAN into CNF would introduce additional pore structures within the fibers, increasing the specific surface area. Indeed, analysis of SEM images showed that the 536-nm and 311-nm diameter fibers for PAN and CNF, respectively, were considerably smaller than the ~8000-nm diameter fibers for CC (Table 1, Fig. 1ADG). Through stabilization and carbonization, the PAN fiber diameters decreased by 42% when converted to CNF; this process was also confirmed by FTIR spectroscopy (SM, Fig. S1). We observed a greater-than-anticipated increase in specific surface area along with a decrease in fiber diameter because we measured an area of 12.35 m^2 g^{-1} for PAN and 108.68 m^2 g^{-1} for CNF (Table 1), representing an 8.8-fold increase. With the decrease in fiber diameter, we anticipated the specific surface area to decrease similarly. This discrepancy implies that considerable specific surface area was introduced through the formation of pore structures during the carbonization process [16]. The specific surface area of CNF was 247-fold larger than that of CC (0.44 m^2 g^{-1}). The conductivity for PAN as a non-carbonized material was negligible, while the conductivity for CNF at 1.12 S cm^{-1} was considerably smaller than that of CC at 57 S cm^{-1} (Table 1).

3.2. PEDOT coating increases specific surface area and conductivity

PEDOT coating increased the fiber diameter for all materials (Table 1). We observed varying coating thicknesses for PAN, CNF, and CC, indicating that materials may have different PEDOT coating affinities. PEDOT appeared to form agglomerates within the PAN mesh increasing the fiber diameter by 24%–666 nm and specific surface area by 46% to 18.07 m^2 g^{-1}. For CNF, we observed a thin, uniform coating of 31 nm (Fig. 1E). PEDOT coating for CNF increased fiber diameter by 10%–342 nm, but surprisingly decreased the specific surface area by 85% to 16.15 m^2 g^{-1}. Thus, the final specific surface area for both PAN and CNF with PEDOT was relatively similar. We had not anticipated this outcome because PEDOT was predicted to add considerable specific surface area [40,41]. For CC, we also observed a thick uniform PEDOT coating of 400 nm (Fig. 1H), resulting in an increase in fiber diameter of 5%–8390 nm, while the specific surface area increased by 95% to 0.86 m^2 g^{-1}. Raman spectroscopy verified that PEDOT had been successfully deposited on all the materials that we tested (SM, Fig. 1CFI).

From these observations, we postulate that PEDOT coating can add considerable specific surface area if the initial substrate surface area is relatively small (smooth). This would explain the increases in specific surface areas for both PAN and CC. The opposite holds true as well; when the substrate contains a considerably large

Table 1
Fiber properties showing fiber diameter, specific surface area, pore size, and conductivity of all materials.

	PAN	PAN with PEDOT (PAN-PEDOT)	CNF	CNF with PEDOT (CNF-PEDOT)	CC	CC with PEDOT (CC-PEDOT)
Fiber diameter (nm)	536 ± 8	666 ± 12	311 ± 4	342 ± 3	$7.99 \times 10^3 \pm 1 \times 10^2$	$8.39 \times 10^3 \pm 8 \times 10^1$
BET surface area (m^2 g^{-1})	12.35 ± 0.18	18.07 ± 0.27	108.7 ± 0.49	16.15 ± 0.2	0.44 ± 0.01	0.86 ± 0.02
Mean pore size (μm)	0.26 ± 0.18	0.3 ± 0.22	0.26 ± 0.19	0.33 ± 0.52	20.8 ± 20.2	26.9 ± 28.7
Conductivity (S cm^{-1})	NA	$7 \times 10^{-3} \pm 4 \times 10^{-4}$	1.12 ± 0.09	3.03 ± 0.01	57 ± 8	89.6 ± 7.6

Please cite this article in press as: J.J.L. Guzman, et al., Journal of Power Sources (2017), http://dx.doi.org/10.1016/j.jpowsour.2017.03.133

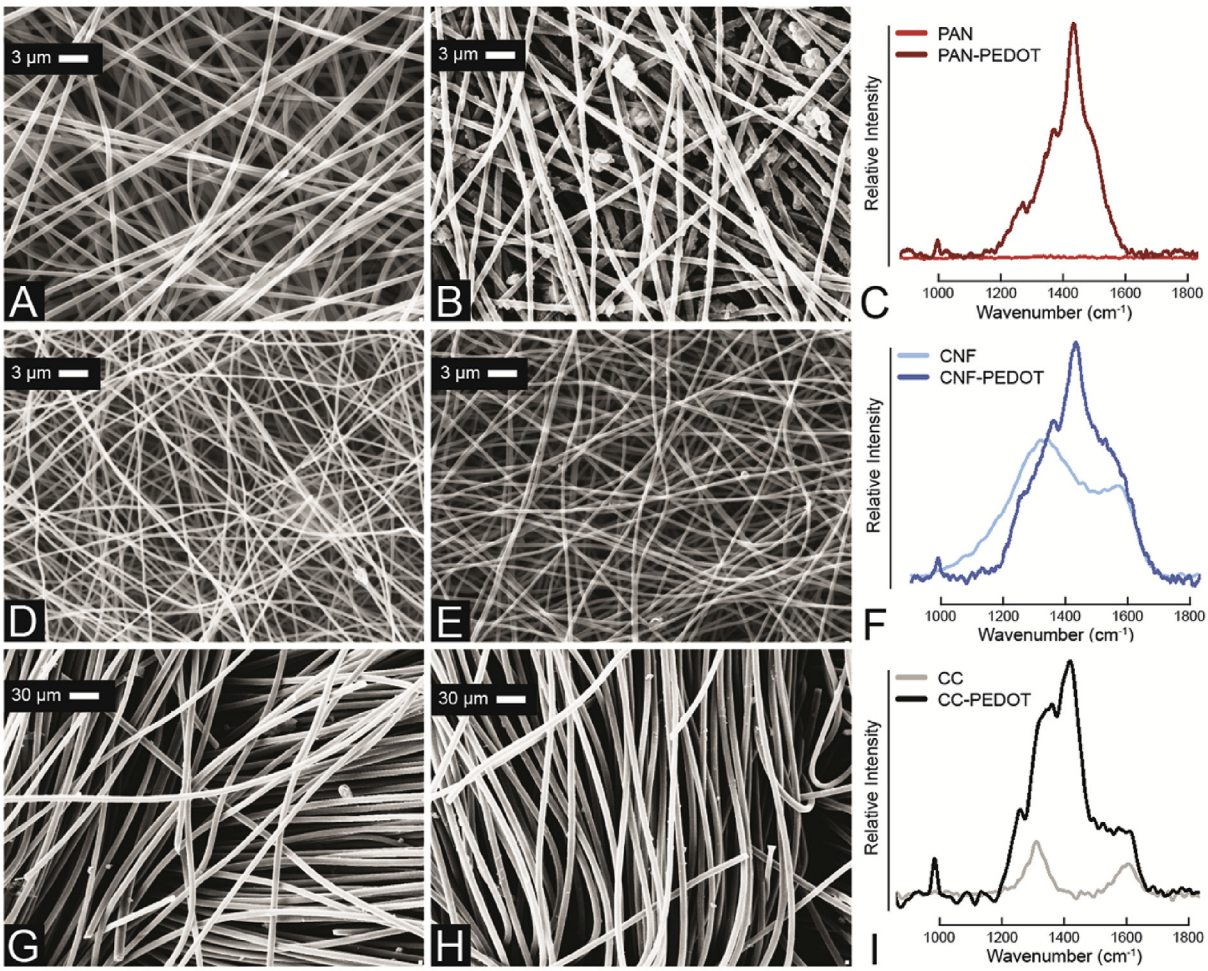

Fig. 1. SEM images of: (A) polyacrylonitrile (PAN); (B) PAN with PEDOT coating (PAN-PEDOT); (D) carbon nanofiber (CNF); (E) CNF with PEDOT coating (CNF-PEDOT); (G) carbon cloth (CC); and (H) CC with PEDOT coating (CC-PEDOT). Raman spectra of: (C) PAN electrodes; (F) CNF electrodes; and (I) CC electrodes.

specific surface area, such as from the pore structures in CNF, PEDOT will essentially clog these structures resulting in a lower surface area. Pore structure and specific surface area are key variables for both electrochemical and bioelectrochemical reactions. PAN and CNF electrodes with and without PEDOT possessed very small pore sizes (0.26–0.33 μm), significantly smaller than that of CC with and without PEDOT (20.8–26.9 μm, respectively) (Table 1). Considering the 0.5 μm width of *G. sulfurreducens* [48], the amount of biologically available specific surface area in PAN and CNF may be limited because some areas may be inaccessible to the cells in the biofilm. Recent studies have shown that if the pore size of a material is too small, cells can be restricted from accessing the full depth and surface area of the material; lowering the biologically-available specific surface area will lead to lower current production [49,50]. Alternatively, the large pore sizes measured with CC could also be limiting, as they have been found to restrict continuous biofilm formation throughout a large fiber mat [14].

PEDOT coating increased the conductivity for all materials tested (Table 1). The conductivity for PAN increased from being entirely nonconductive to a measurable conductivity of 7×10^{-3} S cm^{-1}. CNF increased its conductivity almost 3-fold to 3.03 S cm^{-1} with the addition of PEDOT. CC conductivity increased by 57%–89.6 S cm^{-1} with PEDOT coating. The ability of PEDOT to coat material and increase conductivity and potentially specific surface area shows its promise as a coating for low specific surface area materials.

3.3. PEDOT coating properties increase electrochemical performance

We performed CV under diffusive conditions with ferricyanide mediator under abiotic conditions, and report results normalized to projected surface area (Fig. 2A). We excluded PAN due to its nonconductivity. The conductivity for PAN-PEDOT was high enough to perform CV, and we found that its capacitance was similar to CC — both on an area and mass basis (Fig. 2B, Table S1) — indicating that PEDOT coatings could be explored as a conductive coating on nonconductive substrates. Our CV analysis also showed that for both CNF and CC, electrochemical activity increased significantly after coating with PEDOT. We explain this improvement as a function of the material properties of PEDOT itself, not *per se* by the increase in specific surface area due to the PEDOT coating; after all, the specific surface area for CNF-PEDOT had decreased. CNF-PEDOT performed the best, achieving a capacitance of 1238 F m^{-2}, which was 54% higher than CC-PEDOT (804 F m^{-2}). The capacitance for CC-PEDOT was still considerably higher than for CNF and CC without PEDOT (434 and 286 F m^{-2}, respectively). Without PEDOT, the capacitance for CNF was 52% higher than for CC. The 247-fold greater specific surface area of CNF compared to CC, which we described above, did not have as pronounced of an effect on the capacitance. Possibly, diffusion limitations through the CNF pore structures and the 50-fold lower conductivity could explain the absence of a larger effect on the capacitance.

Please cite this article in press as: J.J.L. Guzman, et al., Journal of Power Sources (2017), http://dx.doi.org/10.1016/j.jpowsour.2017.03.133

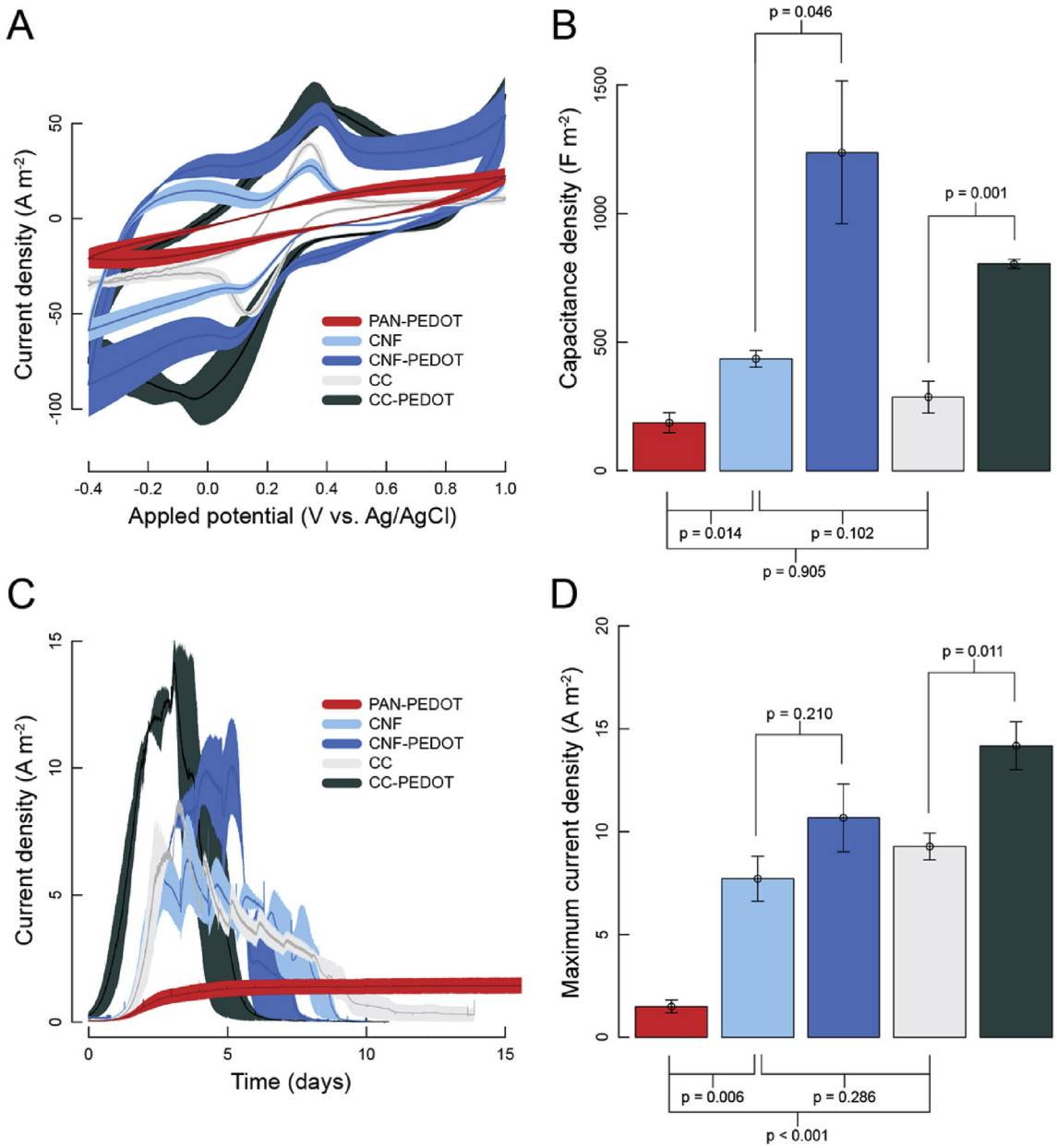

Fig. 2. Cyclic voltammetry (CV) results showing: (A) the averaged CV curves for all materials studied (dark line indicates the mean, shadow indicates standard error); and (B) barplot of the capacitance of each material calculated from the CV curves with statistical analysis. Bioelectrochemical system batch operation results showing: (C) current production during the operating period (dark line indicates the mean, shadow indicates standard error); and (D) barplot of the maximum current production with statistical analysis. All data normalized to projected surface area of electrodes.

3.4. PEDOT coating improves bioelectrochemical performance

In addition to the abiotic CV analysis, the electrode materials were tested in BESs (in triplicate) to determine the compatibility of the material to *G. sulfurreducens*. Since only a small inoculum was used in our BESs, the current produced was related to growth at the electrode (Fig. 2C). The current profiles showed that *G. sulfurreducens* first grew exponentially, and then decreased once acetate (carbon source) had been consumed, because the BESs were operated as batch systems. A periodic pattern in current production was observed throughout the operating period, but this was not related to growth rather related to a laboratory anomaly. We performed a diagnostic CV test daily, which resulted in a repeated hysteresis for the current when the biofilm adjusted back to the normal operating potential. Such hysteresis had not yet been observed in larger BESs that were studied in our lab; this is likely due to the small volume of the BESs.

Due to the nonconductivity of PAN, we did not test this material in a BES. We did test PAN-PEDOT, but it behaved significantly worse than all the other materials, producing only a continuous electric current of 1.50 A m^{-2}. Because of the low growth of *G. sulfurreducens*, the operating period for the PAN-PEDOT batch was more than five weeks with no noticeable decrease in current. Such a long-term operating period indicates a potential to use PEDOT coatings throughout extended operating periods; additional studies with longer operating periods will be necessary to verify, though. For the other materials, we operated the BESs for a little longer than 10 days. Application of PEDOT to the CNF and CC

Please cite this article in press as: J.J.L. Guzman, et al., Journal of Power Sources (2017), http://dx.doi.org/10.1016/j.jpowsour.2017.03.133

electrodes increased their current production by 38% and 64%, respectively (Fig. 2D, Table S2). However, only PEDOT coating on CC resulted in a statistically significant current increase. CC-PEDOT produced the highest current at 15.22 A m^{-2}, while CNF-PEDOT produced a 30% lower current at 10.66 A m^{-2}. CNF and CC performed similar in our BESs at 9.27 and 7.71 A m^{-2}, respectively.

Current production correlated with the increased conductivity and capacitance of the electrodes, rather than with specific surface area. Specific surface area could only explain the increase in performance for CC-PEDOT, yet the benefit was not proportional. PEDOT decreased the specific surface area of CNF by 6.7× times, yet slightly increased current production. While CNF possessed 247× greater specific surface area than CC, CC outperformed CNF in current production. This phenomena has been observed in other studies with simple carbon electrodes, where a chemical process lowered the high specific surface area of an electrode yet increased current production, due to the electrochemical properties the process interred on the surface [51]. Such findings imply that a balance exists between electrode specific surface area and physicochemical properties. With the CNF materials here, this finding assists the likelihood that the small pore structures present in CNF produced measurable high specific surface area which could not be entirely accessed by *G. sulfurreducens*, but the improved material properties from PEDOT allowed for mildly improved current production.

3.5. PEDOT coatings show wide potential of applications

To explore the benefit of using PEDOT as a means to increase current production, we also coated a gold electrode with PEDOT *via* electrodeposition and tested the electrode in a microfluidic BES [52] (SM, Fig. S2A). In this system, the gold electrode was produced through photolithography, producing a mirror-smooth surface with a very low specific surface area, which is theoretically its projected surface area. Using this electrode without PEDOT in a microfluidic BES, *G. sulfurreducens* produced a steady-state current of 8.4 μA throughout an operating period of 5 days (Fig. S2B). When we grew *G. sulfurreducens* on a PEDOT-coated gold electrode, current increased to 23.8 μA, which is a 283% improvement in performance. Subsequent SEM imaging showed a high specific surface area coating selectively attached to the gold electrode. The improved surface features allowed a thicker and more widespread *G. sulfurreducens* biofilm on the PEDOT-coated gold electrode than on the gold electrode (Fig. S3A-F), and confirmed our anticipation that low specific surface area materials (such as *via* photolithography) can be improved considerably by adding a PEDOT coating.

4. Conclusions

Electro-spun carbon nanofiber (CNF) has been explored because of its high porosity, surface area density, biocompatibility, and customizability [14–17]. Notably, CNF features higher specific surface area and porosity compared to conventional electrodes such as graphite, CC, and carbon brush [18–24]. Functionalizing CNF with PEDOT, as performed here, may represent a simple method for improving the performance of BESs. We found that PEDOT increased the current production of CNF by 38% and CC by 64%. In comparison, alternative functionalization methods, such as with platinum or carbon nanotubes, have had 40–50% improvements [25,43,44], but are harder to apply, especially in already existing large-scale systems. Exploring relationships in capacitance, conductivity, and specific surface area, we found that greater conductivity and capacity correlated with bioelectrochemical current production, and that added specific surface area did not play a key role. PEDOT has been shown to increase the specific surface area of materials it coats, but it considerably decreased the area of CNF, which already possessed a high surface area. This implies that materials possessing a high specific surface area, such as from small pores, may not benefit from the added surface area from PEDOT coatings; in fact, PEDOT may lower specific surface area on certain materials. Further, decreases in specific surface area with increases in current production may imply that fine surface features were not biologically available to *G. sulfurreducens*. In an application with a highly smooth gold microelectrode, PEDOT increased current production almost 3-fold, demonstrating the benefit of PEDOT on low specific surface area materials. Even if a material does possess high specific surface area, the benefits of increased conductivity and capacitance appear to show improved performance. This was observed in both the CV and BES tests when PEDOT was added. Employing further studies to quantify optimal PEDOT application quantity can lead to further understanding of this limitation, in addition to selection of proper substrate materials.

Finally, though CNF did not produce as much current in BES tests as CC when normalized to projected surface area, CNF's low density allowed it to outperform CC 5-fold when normalized by mass (Table S2). Mass normalization was not explored in this manuscript because at the point of development, a number of parameters need to be optimized before a fair comparison can be made, such as thickening to increase CNF's rigidity; which could be beneficial, as the CNF materials manufactured here were very thin and fragile. However, thickening will likely affect other key material properties such as porosity and biologically available surface area. Further studies exploring these design parameters will be critical to assess whether CNF can be competitive to CC with and without PEDOT. Finally, long-term BES and MFC tests using continuous flow will be needed to demonstrate whether the electrodes proposed here can be a cost-effective real-world electrode alternative to those already being used today.

Funding

This work has been supported by a HEAA grant and a National Science Foundation Graduate Research Fellowship (#DGE-1144153).

Acknowledgements

This work made use of the Raman microscope, four-point probe conductivity meter, and SEM at the Cornell Center for Materials Research (CCMR) shared facilities, which are supported through the National Science Foundation Materials Research Science and Engineering Centers (MRSEC) program (DMR 1120296). The authors would like to thank Brian Patrick Williams for his support in this study performing BET analysis and Dr. Tianran Sun for assistance with electrochemical analysis (Cornell University). We acknowledge John Grazul, Malcolm G. Thomas, and Barnaby D.A. Levin for assistance with sample preparation and SEM imaging (all at Cornell University).

Glossary

BES	bioelectrochemical system
MFC	microbial fuel cell
PAN	polyacrylonitrile
CNF	carbon nanofiber
CC	carbon cloth
PEDOT	poly(3,4-ethylenedioxythiophene)
SEM	scanning electron microscope
FTIR	Fourier transform infrared
CV	cyclic voltammetry

Please cite this article in press as: J.J.L. Guzman, et al., Journal of Power Sources (2017), http://dx.doi.org/10.1016/j.jpowsour.2017.03.133

Appendix A. Supplementary data

Supplementary data related to this article can be found at http://dx.doi.org/10.1016/j.jpowsour.2017.03.133.

References

[1] S. Gavazza, J.J.L. Guzman, L.T. Angenent, Electrolysis within anaerobic bioreactors stimulates breakdown of toxic products from azo dye treatment, Biodegradation 26 (2015) 151–160.
[2] Z. He, H. Shao, L.T. Angenent, Increased power production from a sediment microbial fuel cell with a rotating cathode, Biosens. Bioelectron. 22 (2007) 3252–3255.
[3] Z. He, L.T. Angenent, Application of bacterial biocathodes in microbial fuel cells, Electroanalysis 18 (2006) 2009–2015.
[4] Z. He, S.D. Minteer, L.T. Angenent, Electricity generation from artificial wastewater using an upflow microbial fuel cell, Environ. Sci. Technol. 39 (2005) 5262–5267.
[5] Z. He, N. Wagner, S.D. Minteer, L.T. Angenent, An upflow microbial fuel cell with an interior cathode: assessment of the internal resistance by impedance spectroscopy, Environ. Sci. Technol. 40 (2006) 5212–5217.
[6] K. Rabaey, L.T. Angenent, U. Schröder, J. Keller, Bioelectrochemical Systems: from Extracellular Electron Transfer to Biotechnological Application, IWA Publishing, London, 2010.
[7] J.J. Fornero, M. Rosenbaum, L.T. Angenent, Electric power generation from municipal, food, and animal wastewaters using microbial fuel cells, Electroanalysis 22 (2010) 832–843.
[8] S. Cheng, D. Xing, D.F. Call, B.E. Logan, Direct biological conversion of electrical current into methane by electromethanogenesis, Environ. Sci. Technol. 43 (2009) 3953–3958.
[9] M. Siegert, M.D. Yates, D.F. Call, X. Zhu, A. Spormann, B.E. Logan, Comparison of nonprecious metal cathode materials for methane production by electromethanogenesis, ACS Sust. Chem. Eng. 2 (2014) 910–917.
[10] L.T. Angenent, M.A. Rosenbaum, Microbial electrocatalysis to guide biofuel and biochemical bioprocessing, Biofuels 4 (2013) 131–134.
[11] B.E. Logan, Scaling up microbial fuel cells and other bioelectrochemical systems, Appl. Microbiol. Biotechnol. 85 (2010) 1665–1671.
[12] D. Pant, A. Singh, G. Van Bogaert, Y.A. Gallego, L. Diels, K. Vanbroekhoven, An introduction to the life cycle assessment (LCA) of bioelectrochemical systems (BES) for sustainable energy and product generation: relevance and key aspects, Renew. Sustain. Energy Rev. 15 (2011) 1305–1313.
[13] J. Wei, P. Liang, X. Huang, Recent progress in electrodes for microbial fuel cells, Bioresour. Technol. 102 (2011) 9335–9344.
[14] S. Chen, G. He, A.A. Carmona-Martinez, S. Agarwal, A. Greiner, H. Hou, U. Schröder, Electrospun carbon fiber mat with layered architecture for anode in microbial fuel cells, Electrochem. Commun. 13 (2011) 1026–1029.
[15] S.S. Manickam, U. Karra, L. Huang, N.-N. Bui, B. Li, J.R. McCutcheon, Activated carbon nanofiber anodes for microbial fuel cells, Carbon 53 (2013) 19–28.
[16] E. Ra, E. Raymundo-Piñero, Y. Lee, F. Béguin, High power supercapacitors using polyacrylonitrile-based carbon nanofiber paper, Carbon 47 (2009) 2984–2992.
[17] W.-X. Zhang, Y.-Z. Wang, C.-F. Sun, Characterization on oxidative stabilization of polyacrylonitrile nanofibers prepared by electrospinning, J. Polym. Res. 14 (2007) 467–474.
[18] H.-Y. Tsai, C.-C. Wu, C.-Y. Lee, E.P. Shih, Microbial fuel cell performance of multiwall carbon nanotubes on carbon cloth as electrodes, J. Power Sources 194 (2009) 199–205.
[19] J. Liu, Y. Qiao, C.X. Guo, S. Lim, H. Song, C.M. Li, Graphene/carbon cloth anode for high-performance mediatorless microbial fuel cells, Bioresour. Technol. 114 (2012) 275–280.
[20] S. Cheng, B.E. Logan, Ammonia treatment of carbon cloth anodes to enhance power generation of microbial fuel cells, Electrochem. Commun. 9 (2007) 492–496.
[21] Y. Luo, F. Zhang, B. Wei, G. Liu, R. Zhang, B.E. Logan, Power generation using carbon mesh cathodes with different diffusion layers in microbial fuel cells, J. Power Sources 196 (2011) 9317–9321.
[22] X. Wang, S. Cheng, Y. Feng, M.D. Merrill, T. Saito, B.E. Logan, Use of carbon mesh anodes and the effect of different pretreatment methods on power production in microbial fuel cells, Environ. Sci. Technol. 43 (2009) 6870–6874.
[23] B. Logan, S. Cheng, V. Watson, G. Estadt, Graphite fiber brush anodes for increased power production in air-cathode microbial fuel cells, Environ. Sci. Technol. 41 (2007) 3341–3346.
[24] Y. Feng, Q. Yang, X. Wang, B.E. Logan, Treatment of carbon fiber brush anodes for improving power generation in air–cathode microbial fuel cells, J. Power Sources 195 (2010) 1841–1844.
[25] A. Deeke, T.H. Sleutels, H.V. Hamelers, C.J. Buisman, Capacitive bioanodes enable renewable energy storage in microbial fuel cells, Environ. Sci. Technol. 46 (2012) 3554–3560.
[26] M. Mustakeem, Electrode materials for microbial fuel cells: nanomaterial approach, Mater. Renew. Sustain. Energy 4 (2015) 22, http://dx.doi.org/10.1007/s40243-015-0063-8.
[27] S. Cheng, H. Liu, B.E. Logan, Power densities using different cathode catalysts (Pt and CoTMPP) and polymer binders (Nafion and PTFE) in single chamber microbial fuel cells, Environ. Sci. Technol. 40 (2006) 364–369.
[28] X. Xie, L. Hu, M. Pasta, G.F. Wells, D. Kong, C.S. Criddle, Y. Cui, Three-dimensional carbon nanotube– textile anode for high-performance microbial fuel cells, Nano Lett. 11 (2010) 291–296.
[29] Y. Zhao, K. Watanabe, K. Hashimoto, Hierarchical micro/nano structures of carbon composites as anodes for microbial fuel cells, Phys. Chem. Chem. Phys. 13 (2011) 15016–15021.
[30] Y. Zou, J. Pisciotta, I.V. Baskakov, Nanostructured polypyrrole-coated anode for sun-powered microbial fuel cells, Bioelectrochemisty 79 (2010) 50–56.
[31] M. Chen, D. Nilsson, T. Kugler, M. Berggren, T. Remonen, Electric current rectification by an all-organic electrochemical device, Appl. Phys. Lett. 81 (2002) 2011–2013.
[32] W.A. Daoud, J.H. Xin, Y.S. Szeto, Polyethylenedioxythiophene coatings for humidity, temperature and strain sensing polyamide fibers, Sens. Actuators B Chem. 109 (2005) 329–333.
[33] H.W. Heuer, R. Wehrmann, S. Kirchmeyer, Electrochromic window based on conducting poly (3, 4-ethylenedioxythiophene)–poly (styrene sulfonate), Adv. Funct. Mater. 12 (2002) 89–94.
[34] J. Niessen, U. Schröder, M. Rosenbaum, F. Scholz, Fluorinated polyanilines as superior materials for electrocatalytic anodes in bacterial fuel cells, Electrochem. Commun. 6 (2004) 571–575.
[35] H. Yamato, M. Ohwa, W. Wernet, Stability of polypyrrole and poly(3,4-ethylenedioxythiophene) for biosensor application, J. Electroanal. Chem. 397 (1995) 163–170.
[36] T.L. Kelly, K. Yano, M.O. Wolf, Supercapacitive properties of PEDOT and carbon colloidal microspheres, ACS Appl. Mater. Interfaces 1 (2009) 2536–2543.
[37] S. Patra, N. Munichandraiah, Supercapacitor studies of electrochemically deposited PEDOT on stainless steel substrate, J. Appl. Polym. Sci. 106 (2007) 1160–1171.
[38] Y. Zhang, H. Feng, X. Wu, L. Wang, A. Zhang, T. Xia, H. Dong, X. Li, L. Zhang, Progress of electrochemical capacitor electrode materials: a review, Int. J. Hydrogen Energy 34 (2009) 4889–4899.
[39] L. Jin, T. Wang, Z.-Q. Feng, M.K. Leach, J. Wu, S. Mo, Q. Jiang, A facile approach for the fabrication of core–shell PEDOT nanofiber mats with superior mechanical properties and biocompatibility, J. Mater. Chem. B 1 (2013) 1818–1825.
[40] Y.L. Kang, S. Ibrahim, S. Pichiah, Synergetic effect of conductive polymer poly(3,4-ethylenedioxythiophene) with different structural configuration of anode for microbial fuel cell application, Bioresour. Technol. 189 (2015) 364–369.
[41] X. Liu, W. Wu, Z. Gu, Poly (3,4-ethylenedioxythiophene) promotes direct electron transfer at the interface between Shewanella loihica and the anode in a microbial fuel cell, J. Power Sources 277 (2015) 110–115.
[42] Y. Wang, C.-E. Zhao, D. Sun, J.-R. Zhang, J.-J. Zhu, A graphene/poly(3,4-ethylenedioxythiophene) hybrid as an anode for high-performance microbial fuel cells, ChemPlusChem 78 (2013) 823–829.
[43] A. Deeke, T.H. Sleutels, A. Ter Heijne, H.V. Hamelers, C.J. Buisman, Influence of the thickness of the capacitive layer on the performance of bioanodes in microbial fuel cells, J. Power Sources 243 (2013) 611–616.
[44] X. Peng, H. Yu, X. Wang, Q. Zhou, S. Zhang, L. Geng, J. Sun, Z. Cai, Enhanced performance and capacitance behavior of anode by rolling Fe_3O_4 into activated carbon in microbial fuel cells, Bioresour. Technol. 121 (2012) 450–453.
[45] J.-H. Kim, A.K. Sharma, Y.-S. Lee, Synthesis of polypyrrole and carbon nanofiber composite for the electrode of electrochemical capacitors, Mater. Lett. 60 (2006) 1697–1701.
[46] L.T. Angenent, Open-source Bond Lab Reactors. http://angenent.bee.cornell.edu/bond.html, 2015 (accessed 1/10/2017).
[47] E. Marsili, J.B. Rollefson, D.B. Baron, R.M. Hozalski, D.R. Bond, Microbial Biofilm Voltammetry: direct electrochemical characterization of catalytic electrode-attached biofilms, Appl. Environ. Microbiol. 74 (2008) 7329–7337.
[48] F. Caccavo, D.J. Lonergan, D.R. Lovley, M. Davis, J.F. Stolz, M.J. McInerney, *Geobacter sulfurreducens* sp. nov., a hydrogen-and acetate-oxidizing dissimilatory metal-reducing microorganism, Appl. Environ. Microbiol. 60 (1994) 3752–3759.
[49] E. Blanchet, B. Erable, M.-L. De Solan, A. Bergel, Two-dimensional carbon cloth and three-dimensional carbon felt perform similarly to form bioanode fed with food waste, Electrochem. Commun. 66 (2016) 38–41.
[50] K. Artyushkova, D. Roizman, C. Santoro, L.E. Doyle, A.F. Mohidin, P. Atanassov, E. Marsili, Anodic biofilms as the interphase for electroactive bacterial growth on carbon veil, Biointerphases 11 (2016) 031013.
[51] M. Epifanio, S. Inguva, M. Kitching, J.-P. Mosnier, E. Marsili, Effects of atmospheric air plasma treatment of graphite and carbon felt electrodes on the anodic current from *Shewanella* attached cells, Bioelectrochemistry 106 (Part A) (2015) 186–193.
[52] Z. Li, A. Venkataraman, M.A. Rosenbaum, L.T. Angenent, A Laminar-flow microfluidic device for quantitative analysis of microbial electrochemical activity, ChemSusChem 5 (2012) 1119–1123.